Catal Lett (2008) 121:63–69
DOI 10.1007/s10562-007-9293-4

Selective Oxidation of Diphenylmethane Over Cobalt Doped Mesoporous Titania–Silica Catalyst with High Ti Content

**Lu Tang · Bin Li · Zhongbiao Zhai · Junjie Li ·
Encai Ou · Jiaqiang Wang**

Received: 3 June 2007 / Accepted: 30 September 2007 / Published online: 12 October 2007

Abstract Cobalt doped mesoporous titania–silica with Ti/Si molar ratio of 0.5 (Co–TiO_2–SiO_2) was synthesized for the oxidation of diphenylmethane in acetic acid using aqueous hydrogen peroxide as oxidant for the first time. Fast hot catalyst filtration experiment proved that the catalyst acted as a heterogeneous one. Recycling of the catalyst indicates that the catalyst can be used a number of times without losing its activity to a greater extent. The effects of reaction time and reaction temperature on the performance of the catalyst were investigated. Moreover, cobalt doped mesoporous titania with a crystalline structure and cobalt doped mesoporous titania–silica with different molar ratio were also studied. It was found that Co–TiO_2–SiO_2 with Ti/Si molar ratio of 0.5 showed the highest activity.

Keywords Oxidation of diphenylmethane · Benzophenone · Co doped mesoporous titania–silica

1 Introduction

Benzophenone (BP) is an important intermediate for perfumes, photo initiators, drugs and pharmaceuticals. The classical synthesis methods such as Friedel–Crafts acylation reactions [1–5] and the use of high oxidation state transition metals for diaryl methyl derivatives oxidation (e.g. CrO_3, $KMnO_4$) [6–8] need critical conditions, and they are expensive, polluting, and risky. Therefore, more and more attention has been transferred to develop a more efficient, easily separable, reusable, and environment-friendly catalyst for the oxidation of diphenylmethane (DPM) to BP [9–12]. It was reported that MnO_4^{-1}-exchanged Mg–Al–hydrotalcite has selectivity and also has an excellent stability and reusability for the oxidation of DPM [9]. Jana and co-works also used Mn–MgAl hydrotalcite for the highly selective oxidation of DPM to BP [10]. Rogovin et al. [11] and Tong et al. [12] prepared BP using cobalt substituted silicate xerogel and *N*-hydroxyphthalimide–acridine yellow–Br_2 system, respectively. Recently we have reported that cobalt doped MCM-41 (Co/MCM-41) presents a highly selective (99.1%) catalyst for the direct oxidation of DPM to benzophenone [13]. But further study found that the color of Co-MCM-41 fade and it had lost some activity after one-run reaction. So far as we know, there is no report on using stable mesoporous catalyst for the oxidation of DPM to BP. Therefore, our aim is to develop a stable mesoporous catalyst for the production of BP.

TiO_2, which is a widely used support, has received great attention in catalysis research over the last two decades. However, titania as a support suffers from limited surface area, poor mechanical strength, a low sintering resistance, and a high cost. To overcome the deficiencies of titania, the composite supports containing titania with silica [14–17] have been proposed. As support, the mixed SiO_2–TiO_2 systems are appearing very attractive to improve the mechanical strength, thermal stability, and surface area of TiO_2. Moreover, these mixed oxides exhibit also interesting properties related to the generation of new catalytic sites for selective oxidation reactions [18].

On the other hand, mesoporous titania materials are of considerable interest as they usually show higher surface

---

L. Tang · B. Li · Z. Zhai · J. Li · E. Ou · J. Wang (✉)
Department of Applied Chemistry, Key Laboratory of Medicinal Chemistry for Natural Resource (Yunnan University), Ministry of Education, Yunnan University, Kunming 650091, P. R. China
e-mail: jqwang@ynu.edu.cn

areas and much more uniform and controllable pore size and pore morphologies compared with randomly organized forms of nanocrystalline titania [19–21]. Very recently, we synthesized cobalt doped mesoporous TiO_2 with a crystalline framework (Co/MTiO_2) and demonstrated that it is efficient catalysts for the oxidation of cyclohexane [22] and *p*-chlorotoluene [23] to cyclohexanol/ cyclohexanone and *p*-chlorobenzaldehyde, respectively, under mild conditions. As described above, the mixed SiO_2–TiO_2 systems are very useful to improve the mechanical strength, thermal stability, and surface area of TiO_2. For example, it has been reported that high loading anatase TiO_2 (30–80 wt.%) were incorporated inside the pores of SBA-15 mesostructured silica host and yielded very high thermostability [24]. However, the information about the size, dispersion, location, and assembling mode of the TiO_2 nanocrystals inside the ordered mesostructured silica was limited and sometimes contradictive, and the synthesis of porous titania–silica mixed metal oxides is still a major challenging task, particularly when high loading and homogeneous distribution titanium species on the SiO_2 support is required [24, 25]. This also resulted in the fact that mesoporous titania–silica with high Ti content (Ti/Si $\geq$ 0.5) and anatase titania framework is very few and there is still rather limited study of the effect of transition metal doping on the mesoporous titania–silica on the oxidation of organic compounds. Although there is a report about using titania–silica catalyst with different Ti content for photocatalytic study [25], so far, up to the authors' knowledge, there is no report on using silica–titania with high Ti content for selective oxidation. Herein, Co doped mesoporous titania–silica with Ti/Si molar ratio of 0.5 (Co–TiO_2–SiO_2) was synthesized and used for selectively catalytic oxidation of DPM to BP for the first time. Co–TiO_2–SiO_2 also shows excellent reusability in the oxidation of DPM to BP.

2 Experimental

2.1 Synthesis of Co–TiO_2–SiO_2

Co–TiO_2–SiO_2 (1 wt.% Co, molar ratio of Ti/Si = 0.5) was synthesized by a modified process as follows: 5.0 g hexadecyltrimethylammonium bromide (CTAB) [$C_{16}H_{33}(CH_3)_3N^+Br^-$] was added to 66 mL solution containing 1.0 g sodium hydroxide. Then, 10 mL tetraethyl orthosilicate (TEOS) was added to it slowly and get a clear gel, finally, the cobalt precursor ($Co(NO_3)_2 \cdot 6H_2O$) and titanium tetraisopropoxide (TTIP) were also alternatively and slowly added to the above gel and stirred for 2 h. The resulting gel was transferred into a Teflon bottle and treated under autogenous pressure without stirring at 363 K for 7 days. The final solid product was filtered, dried, and calcined at 723 K for 24 h.

2.2 Characterization

Pore size distributions, BET surface areas, and pore volumes were measured by nitrogen adsorption/desorption using a NOVA 2000e gas sorption analyzer (Quantachrome Corp.). Prior to the analysis, the samples were degassed at 423 K for ~1 h.

X-ray powder diffraction (XRD) experiments were conducted on a D/max-3B spectrometer with Cu Kα radiation, scans were made in the 2θ range 0.1–5° with a scan rate 0.05°/min (low angle diffraction), and in the 2θ range 10–90° with a scan rate of 10°/min (wide angle diffraction).

FT-IR measurements were performed on a Thermo Nicolet AVATAR FT-IR 360 instrument. Potassium bromide pellets containing 0.5% of the catalyst were used in FT-IR experiments and 34 scans were accumulated for each spectrum in transmission, at a spectral resolution of 4 cm^{-1}. The spectrum of dry KBr was taken for background subtraction.

The laser Raman spectra were measured with a spex1403 spectrometer using the 514.5 nm line of Ar^+ laseremission with a resolution of 1 cm^{-1}.

UV–Vis diffuse reflectance spectra were measured at room temperature in air on a SHIMADZU UV-2401PC photometer over the range from 200 to 800 nm.

Inductively coupled plasma-atomic emission spectrometry (ICP-AES; Labtam Plasma Lab 8440) analysis was used to determine the percentage of metal in the catalysts.

2.3 Oxidation of DPM

For the oxidation of DPM, acetic acid glacial (HAc, AR) as solvent and aqueous hydrogen peroxide (H_2O_2, 30%, AR) as oxidant was used without further purification. The reaction was carried out in a 50 mL two-neck-flask with reflux condenser and magnetically stirred autoclave heated in an oil bath that the temperature could be controlled. The catalyst (50 mg), DPM (500 mg), and HAc (20 mL) were added successively into the two-neck-flask and the aqueous H_2O_2 (2 mL) was added dropwise after the reaction mixture heated to the set temperature. Reaction mixture was filtered under reduced pressure after the set time. Then residue was washed with acetic acid and transferred into the 50 mL volumertric flask. Finally, it was analyzed by high performance liquid chromatography (HPLC) (Agilent 1100 series) with a packed column (kromasil ODS C18 250 × 4.6 mm 5 μm) and an ultraviolet detector (diode array detector). The detector wavelength $\lambda = 254$ nm and temperature of column was 293.15 K. The mobile phase was CH_3OH (chromatographically pure): H_2O = 85:15 (V/V) and the flow rate was 1 mL min^{-1}. The standard substances of DPM and BP were solvated in CH_3OH as standard solution.

3 Results and Discussion

The N_2 adsorption/desorption isotherms of Co–TiO_2–SiO_2 are shown in Fig. 1. The isotherm of Co–TiO_2–SiO_2 can be classified as type IV according to the IUPAC convention and is typical of mesoporous material. This is also supported by the big average pore diameter (5.0 nm), BET surface areas (138 m^2/g), and pore volume (0.17 cm^3/g). Compared with Co doped mesoporous titania with a crystalline framework (Co–$MTiO_2$) [22], the surface area of Co–TiO_2–SiO_2 was increased to 138 m^2/g from 79.8 m^2/g. Obviously, the incorporation of Si into the titania framework improved the surface area. The N_2 adsorption/desorption isotherms of Co–TiO_2–SiO_2 also indicate that the catalyst is not well-ordered which was also observed by the small-angle XRD (not shown). There is only one unobvious peak appeared at 2θ of 0.5–2°, which implies that material has irregular pore channels in the mesoporous region.

The FT-IR spectrum of Co–TiO_2–SiO_2 is depicted in Fig. 2. The bands at ca. 1,090 and ca. 790 cm^{-1} are due to the asymmetric and symmetric Si–O–Si stretching modes, respectively [26]. No bands associated with residual CTAB are observed. For comparison, FTIR spectra of Co-MCM-41 and Co–$MTiO_2$ are also shown in Fig. 3. FTIR spectrum of Co-MCM-41 shows the typical silicate absorptions at about 1081, 806, and 455 cm^{-1}, which can be attributed to Si–O–Si bending and stretching vibrations. While, the FT-IR spectrum of Co–$MTiO_2$ exhibited broad peaks in the range of 400–1,000 cm^{-1} which are contribution from the anatase phase [27–30]. By contrast in this range, it seems that FTIR spectrum of Co–TiO_2–SiO_2 is more like that of Co-MCM-41 other than Co–$MTiO_2$. However, unobvious peaks in the range of 400–1,000 cm^{-1} attributed to the anatase phase [27–30] are found in our sample. Interestingly, in the 1,500–2,000 cm^{-1} region FT-IR spectrum of Co–TiO_2–SiO_2 is different from that of Co-MCM-41 with silica framework but more like that of Co–$MTiO_2$ with titania framework.

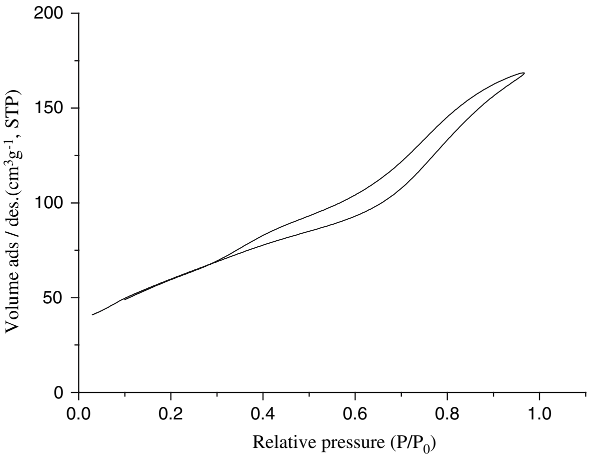

Fig. 1 N_2 adsorption/desorption isotherms of Co–TiO_2–SiO_2

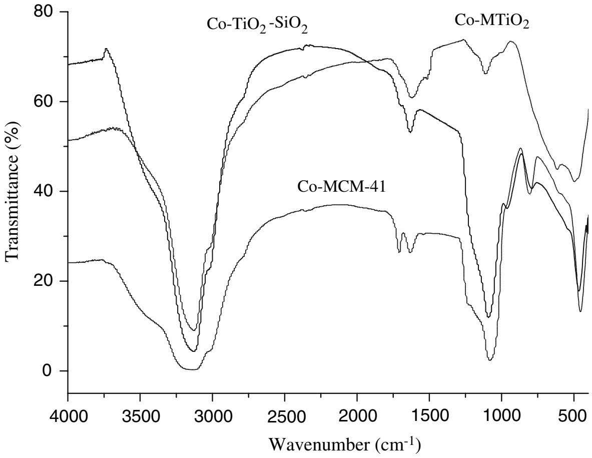

Fig. 2 FT-IR spectra of Co-MCM-41, Co–$MTiO_2$ and Co–TiO_2–SiO_2

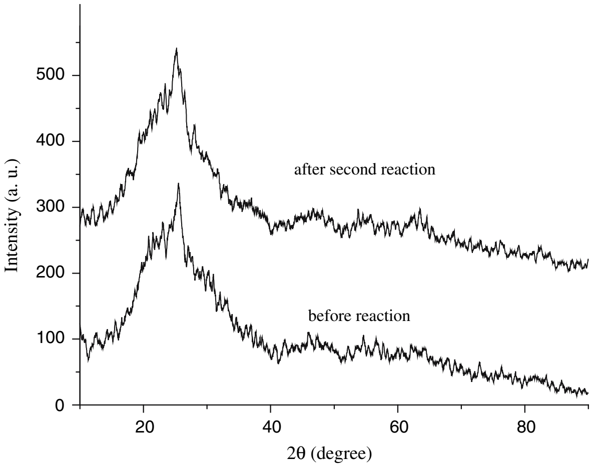

Fig. 3 XRD patterns of Co–TiO_2–SiO_2

Figure 3 shows wide-angle X-ray diffraction (XRD) patterns of Co–TiO_2–SiO_2 measured at 2θ of 10–90°. Wide-angle XRD results showed Co–$MTiO_2$ have anatase crystalline phase [22, 23]. But the incorporation of Si into titania framework made the anatase phase unobvious and it had the characteristic of amorphous silica phase which is consistent with the observation of FTIR spectra.

This is different from that with mass ratio of Ti/Si = 1 reported in ref. [25], where crystalline TiO_2 was clearly observed. Moreover, it is worth noting that no peaks corresponding to the transition metal oxides were observed in our sample. This implies that cobalt is still well dispersed in the titania–silica framework [31].

Raman spectra were measured to determine the structure of TiO_2 in TiO_2–SiO_2. Figure 4 shows the Raman spectra of Co–$MTiO_2$, Co-MCM-41 and Co–TiO_2–SiO_2. The Raman spectra of Co–TiO_2–SiO_2 is some like that of Co–$MTiO_2$ but very different from that of Co-MCM-41. Co–TiO_2–SiO_2 shows four bands at 155, 256, 403, 513, and 632 cm^{-1}, and the intensity of the band at 155 cm^{-1} is extremely strong which is similar to that of anatase [32, 33]. Compared with the peak at 143 cm^{-1} of anatase TiO_2 [32, 33], the peaks of both Co–$MTiO_2$ and Co–TiO_2–SiO_2 shift to 155 cm^{-1}. The red-shift indicates the interaction between the titania and the Co ions present in the mesoporous framework [34]. Compared with that of Co–$MTiO_2$, all the bands are wider and all the bands, except for that at 155 cm^{-1}, are much weaker. This may be attributed to the incorporation of Si into titania framework which is further proved by the small band at 967 cm^{-1} attributable to the Ti–O–Si species [35]. Same as the observations by XRD, no peaks corresponding to the transition metal oxides were observed in our sample indicating that the Co ions are well dispersed in the titania–silica framework.

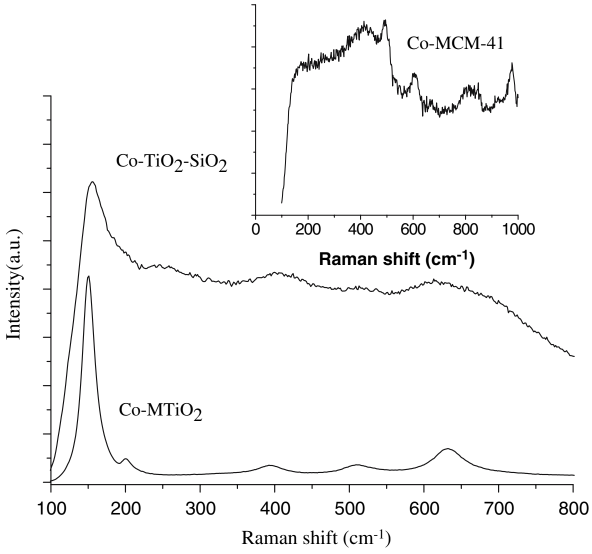

Fig. 4 Raman spectra of Co-MCM-41, Co–$MTiO_2$ and Co–TiO_2–SiO_2

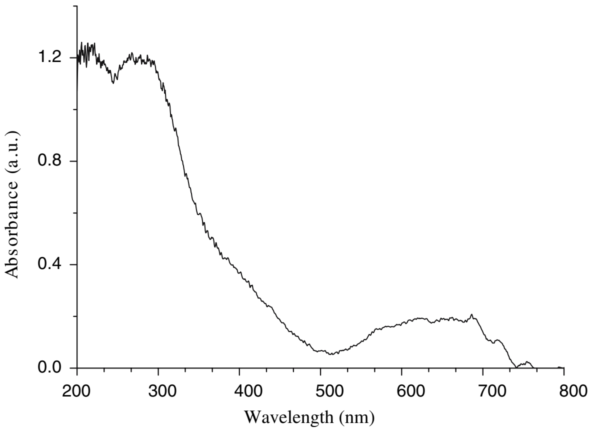

Fig. 5 UV–Vis diffuse reflectance spectra of Co–TiO_2–SiO_2

The diffuse reflectance UV–Vis spectroscopy was known to be a very sensitive probe for the identification and characterization of metal ion coordination and its existence in the framework and/or in the extra-framework position of metal containing zeolites [36]. The diffuse reflectance UV–Vis spectrum of Co–TiO_2–SiO_2 given in Fig. 5 showed two bands with the maxima near 320 and 220 nm attributed to the $O^{2-} \rightarrow Ti^{4+}$ [37]. Incorporation of cobalt resulted in a shoulder near 400 nm, with a broad peak around 600 nm. While the absorption at 400 nm indicated the presence of Co^{3+}, the absorption at 500–750 nm can be attributed to the presence of both Co^{2+} and Co^{3+} [16, 37]. The position of this peak over 500–750 nm is a little different from that of Co–TiO_2–SiO_2 aerogels which was prepared by sol–gel method instead of templating method [16]. The reason is probably due to the different preparation method and the significantly higher TiO_2 loading for our sample.

Using Co–TiO_2–SiO_2 as a catalyst, it was found that BP was the major product, and only small amounts of other products, viz. 2-hydroxybenzophenone (2-HOBP), 2-benzylphenol, diphenylmethanol were observed for the oxidation of DPM. The nature of solvents was known to have a major influence on reaction kinetics and product selectivity in the oxidation of DPM. It has been reported that acetic acid does not only act as a solvent, but also serves as a good oxidizing agent because of the formation of the framework titanium–peracetic acid complex when it reacts with hydrogen peroxide in the presence of titanium-containing zeolites (TS-1) [38–40]. Furthermore, it has been found that Co–$MTiO_2$ [22, 23], Ce-MCM-41 [41] and Co-MCM-41 [13] exhibited high activity when using acetic acid as a solvent [13, 22, 23, 41]. So we also used acetic acid as a solvent for the oxidation of DPM.

The effect of reaction temperature on DPM reaction over Co–TiO_2–SiO_2 is shown in Fig. 6. It is clear that the conversion of DPM was found to increase with increase in reaction temperature and passed through a maximum at 373 K. A further increase in the reaction temperature resulted in slightly increase in the conversion rate of DPM but significant decrease in the selectivity of BP, probably owing to a quicker decomposition of H_2O_2 and the increase in the activity of the catalyst at higher temperature which

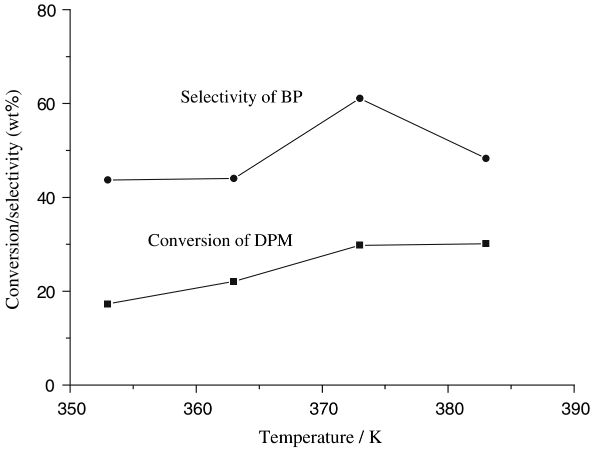

Fig. 6 Effect of temperature on the conversion and selectivity over Co–TiO_2–SiO_2 (Reaction conditions: 20 mL acetic acid; 2 mL H_2O_2 (30%); reaction time, 4 h; catalyst, 0.05 g)

result in the further oxidation of BP to 2-HOBP. Considering the effect of temperature on both conversion of DPM and selectivity of BP, 373 K was chosen as the suitable temperature for the oxidation of DPM.

The effect of reaction time on DPM reaction over Co–TiO_2–SiO_2 was also investigated and depicted in Fig. 7. It is seen that the conversion of DPM increased with time up to 10 h while the selectivity of BP reached the highest when the reaction time was 8 h. Therefore, the optimum conversion and selectivity could be achieved at about 8 h.

For comparisons, we studied the oxidation of DPM using TiO_2–SiO_2(Ti/Si molar ratio of 0.5)with out the incorporation of Co, Co doped mesoporous titania with a crystalline framework (Co–MTiO_2) and different molar ratio of Co-TiO_2-SiO_2 (Ti/Si molar ratio of 0.4 and 0.6)as catalysts under the optimum conditions with those used for Co–TiO_2–SiO_2 (Ti/Si molar ratio of 0.5). These comparisons are summarized in Table 1. As expect, TiO_2–SiO_2 without doped by cobalt did not show any significant activity just similar to the result of those without adding catalyst. This indicates that in Co-TiO_2-SiO_2, the active component was cobalt. Furthermore, it is apparent that the incorporation of Si into the titania framework significantly enhanced the activity of reaction of DPM compared with Co–MTiO_2. In particular, the selectivity of BP was increased by a factor about 1.5 when Co–TiO_2–SiO_2 with Ti/Si molar ratio of 0.5 was compared with Co–MTiO_2. In comparison with the lower selectivity of BP using Co–MTiO_2 as a catalyst and much higher selectivity of BP using Co-MCM-41 [13] as a catalyst, reasonable selectivity of BP between them was obtained using Co–MTiO_2 as a catalyst. Moreover, Co–TiO_2–SiO_2 with Ti/Si molar ratio of 0.4 and 0.5 exhibits the similar conversion and selectivity while the conversion of DPM increased with the increase of the Ti/Si molar ratio. Furthermore, the significant decrease in the selectivity of BP when the molar ratio of Ti/Si was increased to 0.6 may be due to the decrease in surface area of the catalyst. However, the situation must be more complicated than a surface area phenomenon because the high surface area, the extent of dispersion, and local structure of the metal oxides are beneficial for enhancing the reaction. Maybe 0.5 is the optimum Ti/Si molar ratio for Co–TiO_2–SiO_2. Interestingly, using Co-MCM-41 as a catalyst, a byproduct 2-hydroxybenzophenone (2-HOBP) showed a selectivity of higher than 5% [10], by contrast, only little 2-HOBP was detected when using Co–TiO_2–SiO_2 as a catalyst. The high efficiency of Co–TiO_2–SiO_2 (Ti/Si molar ratio of 0.5) may be explained as follows: Firstly, Ti/Si materials would take advantage of both TiO_2 (an n-type semiconductor and active catalyst support) and SiO_2 (high thermal stability and excellent mechanical strength) [35]. Secondly, Co-doped mesoporous materials

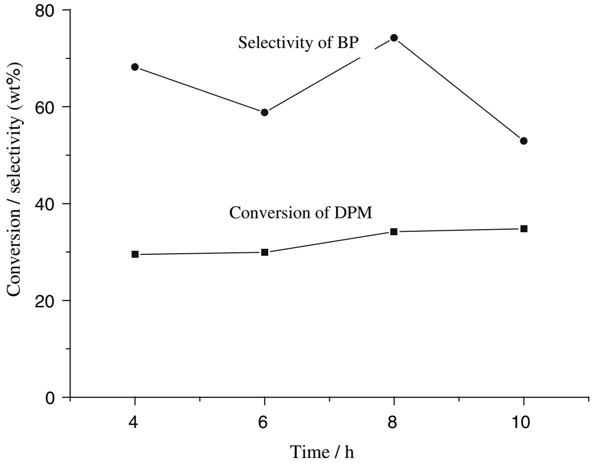

Fig. 7 Effect of reaction time on the conversion and selectivity over Co–TiO_2–SiO_2 (Reaction conditions: 20 mL acetic acid; 2 mL H_2O_2 (30%); reaction temperature, 373 K; catalyst, 0.05 g)

Table 1 Comparison of catalytic activities of different catalysts for the oxidation of DPM to BP

Catalyst	Conversion of DPM(%)	Selectivity to BP(%)
Co–MTiO_2	23.4	47.8
Co–TiO_2–SiO_2^a	31.5	71.0
Co–TiO_2–SiO_2^b	34.2	74.2
Co–TiO_2–SiO_2^c	38.2	50.5
TiO_2–SiO_2^a	22.4	43.4
First recycle	32.3	70.8
Second recycle	31.9	71.2

Superscripts a, b, and c: Ti/Si molar ratio is 0.4, 0.5, and 0.6, respectively. Reaction conditions: 0.5 g DPM; 0.05 g catalyst; 8 h reaction time; 2 mL H_2O_2 (30%); 20 mL acetic acid as solvent; 373 K for reaction temperature still have monodispersed, single-pore distributed, huge pore volume and highly ordered mesoporous structures [22] which are excellent activity for catalysis. Thirdly, the reasonable activity of Co–TiO_2–SiO_2 is due to not only the presence cobalt ions and the interactions between cobalt, titanium, and silica but also the special structure of Co–TiO_2–SiO_2. These findings are not clearly understood yet, and further experiments are underway.

In order to prove that whether the catalyst is a heterogeneous one, experiments with fast hot catalyst filtration and studying the reactivity of the filtrate had been done by a modified process as Ref. [42]: 50 mg catalyst, 20 mL HAc and 2 mL H_2O_2 was stirred at the temperature of 373 K for one hour, then quickly filtrate the catalyst. Let the filtration to react further with DPM by adding 2 mL H_2O_2. The reaction carried out using this filtrate confirmed the absence of active metal ions as it exhibited only similar conversion of DPM (22.3%) and selectivity of BP (43.4%) with those without adding any catalyst. This observation was also well supported by ICP-AES analysis of the filtrates obtained from the fast hot catalyst filtration where negligible amount of leaching of active cobalt and titanium species ($\leq$0.001 wt%) was detected. These indicated that the active component (cobalt) did not leach to the solution and the Co–TiO_2–SiO_2 did act as a heterogeneous catalyst.

To study the stability and recycling ability of Co–TiO_2–SiO_2 under reaction conditions, recycling experiment were carried out. The reactions were also under the optimum conditions with those used for Co–TiO_2–SiO_2. The typical recycling procedure was as follows: after the initial reaction, the catalyst was separated from the reaction mixture and washed with acetone and dried at 363 K, followed by the activation at 723 K for 4 h. The catalyst Co–TiO_2–SiO_2 showed excellent reusability in the oxidation reactions. The conversion of DPM and the selectivity of BP changed little: the selectivity of BP was still higher than 70%. In order to check the structure of the catalyst after each reaction, XRD patterns (Fig. 3) were recorded and clearly indicated that the catalysts, before and after reaction, show the same reflections characteristic of amorphous silica phase.

The present study indicates that the catalyst can be recycled a number of times without loosing its activity to a greater extent. The reason for the better recycling ability of Co–TiO_2–SiO_2 than Co-MCM-41 may be that the incorporation of titania leads to an increase in stability when using acetic acid as solvent compared to compounds such as pure silica or pure titania.

4 Conclusions

In conclusion, Co-TiO_2-SiO_2 was an efficient catalysis for the oxidation of DPM under relatively mild reaction conditions without adding any initiator. Fast hot catalyst filtration experiment proved that the catalyst acted as a heterogeneous one. Recycling of the catalyst indicates that the catalyst can be used a number of times without losing its activity to a greater extent. Its applications in the selective oxidation of other similar compounds are underway.

Acknowledgments The authors thank the National Natural Science Foundation of China (Project 20463003) and Natural Science Foundation of Yunnan Province (Project 2004E0003Z) for financial support. We also thank Center for Advanced Studies of Medicinal and Organic Chemistry, Yunnan University for partial financial support.

References

1. Khadilkar BM, Borkar SD (1997) Tetrahedron Lett 38:1641
2. Tagawa T, Amemiya J, Goto S (2004) Appl Catal A 257:19
3. Jacob B, Sugunan S, Singh AP (1999) J Mol Catal A: Chem 139:43
4. Patil PT, Malshe KM, Kumar P, Dongare MK, Kemnitz E (2002) Catal Commun 3:411
5. Bezouhanova CP (2002) Appl Catal 229:127
6. Borkar SD, Khadilkar BM (1999) Synth Commun 29:4295
7. Shaabani A, Bazgir A, Teimouri F, Lee DG (2002) Tetrahedron Lett 43:5165
8. Clark JH, Kybett AP, Landon P, Macquarrie DJ, Martin K (1989) J Chem Soc, Chem Commun 1355
9. Choudhary VR, Indurkar JR, Narkhede VS (2004) J Catal 227:257
10. Jana SK, Kubota Y, Tatsumi T (2007) J Catal 247:214
11. Rogovin M, Neumann R (1999) J Mol Catal A: Chem 138:315
12. Tong X, Xu J, Miao H, Gao J (2006) Tetrahedron Lett 47:1763
13. Chang F, Li W, Xia F, Yan Z, Xiong J, Wang J (2005) Chem Lett 34:1540
14. Galan-Fereres M, Mariscal R, Alemany LJ, Fierro JLG, Anderson JA (1994) J Chem Soc, Faraday Trans 90:3711
15. Baiker A, Dollenmeier P, Glinski M, Reller A (1987) Appl Catal 35:365
16. Wang J, Uma S, Klabunde KJ (2004) Appl Catal B 48:151
17. Reddy B, Mehdi S, Reddy E (1993) Catal Lett 20:317
18. Boccuzzi F, Coluccia S, Martra G, Ravasioy N (1999) J Catal 184:316
19. Antonelli D, Ying J (1995) Angew Chem Int Ed Engl 34:2014
20. Yang P, Zhao D, Margolese D, Chmelka B, Stucky DG (1999) Chem Mater 11:2813
21. Yue Y, Gao Z (2000) Chem Commun 1755
22. Yao W, Fang H, Ou E, Wang J, Yan Z (2006) Cata Commun 7:387
23. Wang J, Fang H, Li Y, Li J, Yan Z (2006) J Mol Catal A: Chem 250:75
24. Landau MV, Vradman L, Wang X, Titelman L (2005) Micropor Mesopor Mater 78:117
25. Zhang X, Zhang F, Chan K-Y (2005) Appl Catal A Gen 284:193
26. Zeleňák V, Hornebecq V, Mornet S, Schäf O, Llewellyn P (2006) Chem Mater 18:3184
27. Peng T, Zhao D, Song H, Yan C (2005) J Mol Catal A: Chem 238:119
28. Soler-Illia G, Louis A, Sanchez C (2002) Chem Mater 14:750
29. Yu J, Zhang L, Zheng Z, Zhao J (2003) Chem Mater 15:2280
30. Karakitsou K, Verykios X (1993) J Phys Chem 97:1184
31. Wang J, Uma S, Klabunde KJ (2004) Micropor Mesopor Mat 75:143

32. Tanaka T, Teramura K, Yamamoto T, Takenaka S, Yoshida S, Funabiki T (2002) J Photochem Photobio A 148:277
33. Srinivasan S, Datye A, Smith M, Wachs I, Deo G, Jehng J, Turek A, Peden C (1991) J Catal 131:260
34. Rodrigues S, Ranjit K, Uma S, Martyanov I, Klabunde KJ (2005) Adv Mater 17:2467
35. Gao X, Wachs I (1999) Catal Today 51:233
36. Laha SC, Mukherjee P, Sainkar SR, Kumar R (2002) J Catal 207:213
37. Brik Y, Kacimi M, Ziyad M, Verduraz F (2001) J Catal 202:118
38. Sooknoi T, Limtrakul J (2002) Appl Catal A 233:227
39. Velusamy S, Punniyamurthy T (2003) Tetrahedron Lett 44:8955
40. Sato T, Dakka J, Sheldon R (1994) J Chem Soc Chem Commun 16:1887
41. Yao W, Chen Y, Min L, Fang H, Yan Z, Wang H, Wang J (2005) J Mol Catal A Chem 246:161
42. Sheldon R, Wallau M, Arends I, Schuchardt U (1998) Acc Chem Res 31:485